Peer-reviewed version available at Quaternary 2019, 2, 6; doi:10.3390/quat2010006

*Review*

# Late Quaternary variations in the South American Monsoon System as inferred by speleothems – new perspectives using the SISAL database

**Michael Deininger [1*], Brittany Marie Ward [2], Valdir F. Novello [3], Francisco W. Cruz [3]**

[1] Institute of Geosciences, Johannes Gutenberg University Mainz, J.-J.-Becher-Weg 21, 55128 Mainz, Germany
[2] Faculty of Science and Engineering, The University of Waikato, Private Bag 3105, Hamilton 3240, New Zealand
[3] Institute of Geosciences, University of São Paulo, Rua do Lago 562, São Paulo, Brazil
* Correspondence: michael.deininger@uni-mainz.de

**Abstract:** Here we present an overview of speleothem $\delta^{18}O$ records from South America, which mostly are available in the Speleothem Isotopes Synthesis and Analysis (SISAL_v1) database. South American tropical and subtropical $\delta^{18}O$ time series are primarily interpreted as being driven by the amount effect and, consequently show the past history of the convection intensity of convergence zones such as the Intertropical Convergence Zone and the South America Monsoon System. We investigate past hydroclimate scenarios in South America related to the South American Monsoon System in three different time scales: Late Pleistocene, Holocene and the last two millennia. The precession driven insolation is the main driver of convective variability over the continent during the last 250 kyrs, including the Holocene period. However a dipole is observed between the west and east portions of the continent. Records located in the central region of Brazil appear to be weakly affected by insolation driven variability and more susceptible to the South Atlantic Convergence Zone. Cold episodic events in Northern Hemisphere increase the activity of the South American Monsoon System on all time scales, in turn increasing rainfall amounts in South America, as was documented during Heinrich events in the late Pleistocene and Bond events in the Holocene, as well as during the Little Ice Age.

**Keywords:** South American Monsoon System; SAMS; SISAL; speleothems; Quaternary

## 1. Introduction

Rainfall variability in South America is primarily driven by the Intertropical Convergence Zone (ITCZ) [1] and the South American Monsoon System (SAMS) [2], which in turn is influenced, between other forcings, by South Atlantic cyclones (SACs), the Southern Hemisphere (SH) westerly winds (SHWW) and sea surface temperatures of the ancient Atlantic and Pacific Ocean. To gain a deeper understanding of these past variations, it is essential to reconstruct past climate changes of the South American hydroclimate in space and time, infer regional and continental teleconnections from these reconstructions and to identify the underlying climate mechanism. This is not only important for predictions of future changes of the South American hydroclimate in response to global warming, but also to decipher the ecological and biogeographical response to these past changes, such as from the Amazon rainforest, Pantanal, caatinga (Brazilian savanna), cerrado and Atlantic forests, which together, contains one of the richest region of biodiversity on Earth. One rich archive of past changes in the South American hydroclimate are speleothems. The SISAL database/initiative [3] is therefore a major contribution towards these aims, because it aims to collect all available speleothems data allowing to conduct spatio-temporal analysis of time slices or time periods, to compare new reconstructions with existing speleothem datasets (which is apparently much easier if all available reconstructions are archived in one single database) or to test new concepts.

Preprints (www.preprints.org) | NOT PEER-REVIEWED | Posted: 5 October 2018 doi:10.20944/preprints201810.0094.v1

Peer-reviewed version available at Quaternary 2019, 2, 6; doi:10.3390/quat2010006

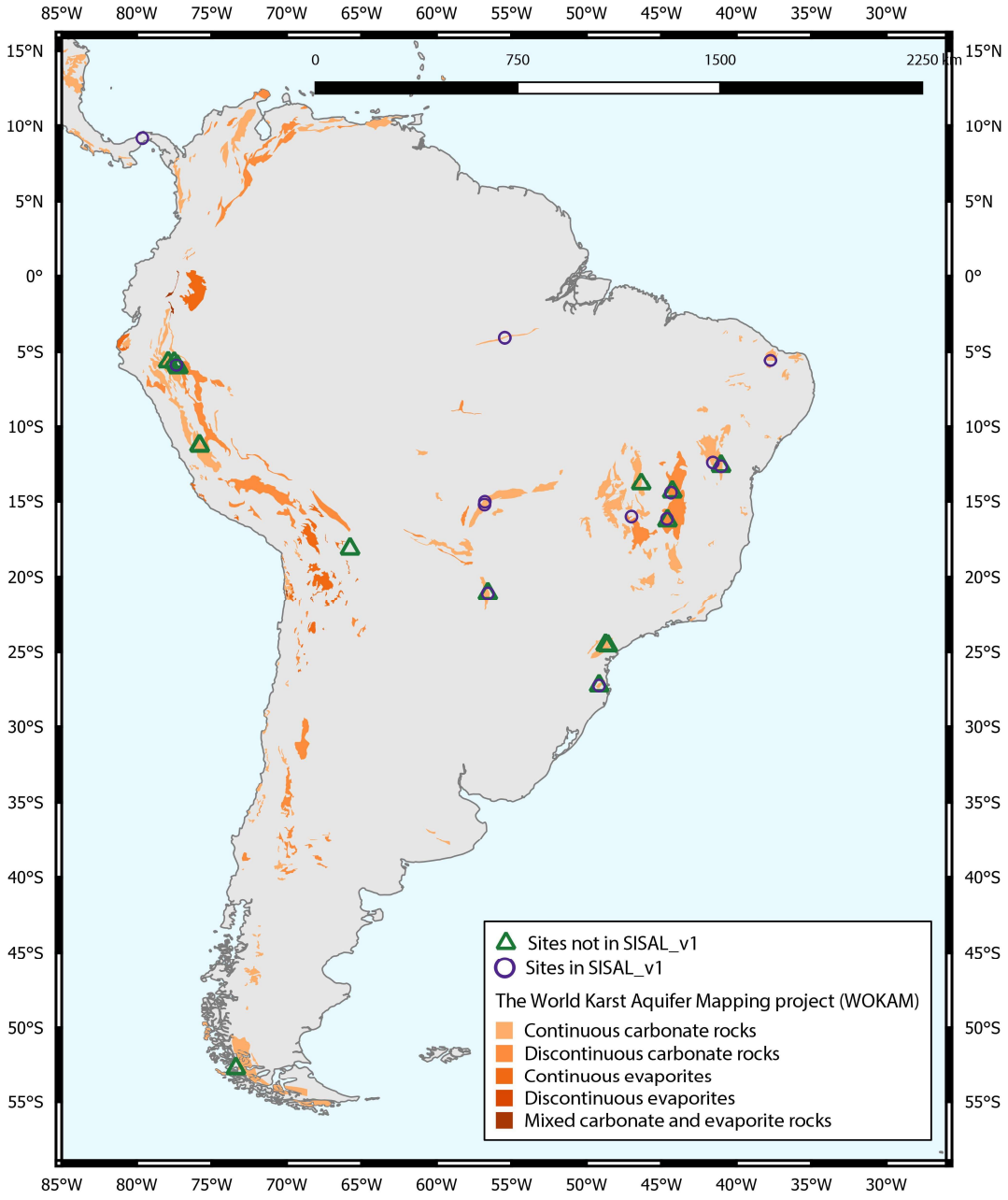


**Figure 1.** Map showing distribution of carbonate and evaporite rocks in South America, provided by the World Karst Aquifer Mapping project (WOKAM [4]). Green triangles indicate study sites in the region identified by the SISAL working group but not included yet, while purple circles show sites that are already in SISAL_v1. Specific information on sites and entities are listed in Table 1.

Speleothem-based reconstructions from South American are distributed over the entire continent ranging from the tropical climate of Venezuela in the North to the chilly climate of Patagonia at the southern tip of South America, as well, from the wet and cold climates of the Andes in the West thought the tropical climate in the Amazonas to the dry climate of Nordeste, respectively (Figure 1). However, despite this continental coverage, currently, all records that are included in SISAL_v1 are located in the tropical and sub-tropical climate zones of central and southeastern Brazil that are influenced mainly by the SAMS. For this reason, this review is focused mainly on past variations of the SAMS that are revealed by speleothem $\delta^{18}O$ time series ($\delta^{18}O$ states the ratio of 18-oxygen ($^{18}O$) to 16-oxygen in carbonates relative to the VPDB standard). The interpretation of speleothem $\delta^{18}O$ is, compared to other regions, straightforward, because it is determined either by

Preprints (www.preprints.org) | NOT PEER-REVIEWED | Posted: 5 October 2018 doi:10.20944/preprints201810.0094.v1

Peer-reviewed version available at Quaternary 2019, 2, 6; doi:10.3390/quat2010006

the amount effect, which describes the negative relationship between rainfall amount and speleothem $\delta^{18}O$ (i.e. $\delta^{18}O$ decreases if rainfall amount increases) [5] or by a pronounced source effect in southeastern Brazil related to moisture that origins from the Amazon basin (low $\delta^{18}O$ values) or the adjacent South Atlantic ocean (high $\delta^{18}O$ values) [6,7]. These two major processes determining speleothem $\delta^{18}O$ values for most of the discusses speleothem $\delta^{18}O$ time series and exceptions are clearly stated in the discussion of individual speleothem $\delta^{18}O$ time series if necessary.

**Table 1.** Cave sites (name and id in SISAL) and entities (name and id in SISAL) of speleothems in South America. Cave sites and entities that are included in SISALv1 have a unique identifier (id) whereas the id is empty if cave sites and entities are not included yet. Min and max year state the youngest and oldest age of the isotope time series in the SISAL_v1 database. Furthermore, headers that are *italic* (e.g. *Site name*) are variables in SISAL_v1 database.

| *Site_name* | *Side_id* | Country | *Entity_name* | *Entity_id* | *Latitude °N* | *Longitude °E* | Min Year BP | Max Year BP | Reference |
|---|---|---|---|---|---|---|---|---|---|
| Abissal cave | 18 | Brazil | Abissal | 79 | -5,6 | -37,73 | 24164 | 25694 | [8] |
| Abissal cave | 18 | Brazil | Ale-1 | 80 | -5,6 | -37,73 | 15057 | 17199 | [8] |
| Botuverá cave | 144 | Brazil | BTV21a | 311 | -27,22 | -49,16 | 196 | 9211 | [9] |
| Botuvera cave | 144 | Brazil | BT2 | 312 | -27,22 | -49,16 | -55 | 116100 | [6] |
| Botuvera cave | 144 | Brazil | BTV4A | | -27,22 | -49,16 | | | [10] |
| Botuvera cave | 144 | Brazil | BTV4C | | -27,22 | -49,16 | | | [10] |
| Botuvera cave | 144 | Brazil | BT3A | | -27,22 | -49,16 | | | [11] |
| Cascayunga cave | | Peru | CAS-A | | -6,09 | -77,22 | | | [12] |
| Cascayunga cave | | Peru | CAS-D | | -6,09 | -77,22 | | | [12] |
| Chiflonkhakha cave | | Bolivia | Boto1 | | -18,12 | -65,77 | 234 | 375 | [13] |
| Chiflonkhakha cave | | Bolivia | Boto3 | | -18,12 | -65,77 | 180 | 1106 | [13] |
| Chiflonkhakha cave | | Bolivia | Boto7 | | -18,12 | -65,77 | 91 | 315 | [13] |
| Chilibrillo cave | 78 | Panama | CHIL-1 | 167 | 9,17 | -79,62 | 690 | 2180 | [14] |
| Cristal cave | | Brazil | CR1 | | -24,58 | -48,58 | | | [5] |
| Cueva Del Diamante | | Peru | NAR-C | | -5,73 | -77,5 | | | [15] |
| Cueva Del Diamante | | Peru | NAR-D | | -5,73 | -77,5 | | | [15] |
| Cueva Del Diamante | | Peru | NAR-F | | -5,73 | -77,5 | | | [15] |
| Cueva del Tigre Perdido | | Peru | NC-A | | -5,94 | -77,31 | | | [16] |
| Cueva del Tigre Perdido | | Peru | NC-B | | -5,94 | -77,31 | | | [16] |
| Curupira cave | 35 | Brazil | CUR4 | 110 | -15,02 | -56,78 | -21 | 154,85 | [17] |
| Diva cave | 38 | Brazil | DV2 | 113 | -12,37 | -41,57 | 39 | 2765 | [18] |
| El Condor cave | | Peru | ELC-A | | -5,93 | -77,3 | | | [15] |
| El Condor cave | | Peru | ELC-B | | -5,93 | -77,3 | | | [15] |
| Huagapo Cave | | Peru | P00-H1 | | -11,27 | -75,79 | | | [19] |
| Huagapo Cave | | Peru | P09-H2 | | -11,27 | -75,79 | | | [19] |
| Jaragua cave | 10 | Brazil | JAR7 | 55 | -21,08 | -56,58 | 5489 | 18596 | [20] |
| Jaragua cave | 10 | Brazil | JAR14 | 56 | -21,08 | -56,58 | 15331 | 22305 | [20] |
| Jaragua cave | 10 | Brazil | JAR13 | 57 | -21,08 | -56,58 | 21852 | 27906 | [20] |
| Jaraguá cave | | Brazil | JAR4 | | -21,08 | -56,58 | -50 | 760 | [21] |
| Jaraguá cave | | Brazil | JAR1 | | -21,08 | -56,58 | 499 | 1508 | [21] |
| Lapa Doce cave | 103 | Brazil | LD12 | 203 | -12,37 | -41,57 | -61 | 39 | [21] |

Preprints (www.preprints.org) | NOT PEER-REVIEWED | Posted: 5 October 2018 doi:10.20944/preprints201810.0094.v1

Peer-reviewed version available at Quaternary 2019, 2, 6; doi:10.3390/quat2010006

| | | | | | | | | |
|---|---|---|---|---|---|---|---|---|
| Lapa Grande | | Brazil | LG3 | | -14,36 | -44,28 | | | [22] |
| Lapa Grande | | Brazil | LG11 | | -14,36 | -44,28 | | | [22] |
| Lapa Grande | | Brazil | LG12B | | -14,36 | -44,28 | | | [23] |
| Lapa Grande | | Brazil | LG19 | | -14,36 | -44,28 | | | [23] |
| Lapa Grande | | Brazil | LG25 | | -14,36 | -44,28 | | | [23] |
| Lapa Sem Fim | | Brazil | LSF3 | | -16,26 | -44,6 | | | [23] |
| Lapa Sem Fim | | Brazil | LSF9 | | -16,26 | -44,6 | | | [23] |
| Lapa Sem Fim | | Brazil | LSF11 | | -16,26 | -44,6 | | | [23] |
| Lapa Sem Fim | | Brazil | LSF13 | | -16,26 | -44,6 | | | [23] |
| Lapa Sem Fim | | Brazil | LSF15 | | -16,26 | -44,6 | | | [23] |
| Lapa Sem Fim | | Brazil | LSF16 | | -16,26 | -44,6 | | | [23] |
| Lapa sem fim cave | 24 | Brazil | LSF16 | 91 | -16,15 | -44,63 | 14373 | 18168 | [24] |
| Lapa sem fim cave | 24 | Brazil | LSF3 | 92 | -16,15 | -44,63 | 17296 | 19304 | [24] |
| MA Cave | | Chile | MA-1 | | -52,68 | -73,38 | | | [25] |
| MA Cave | | Chile | MA-2 | | -52,68 | -73,38 | | | [25] |
| MA Cave | | Chile | MA-3 | | -52,68 | -73,38 | | | [25] |
| Marota Gigante cave | | Brazil | MAG | | -12,58 | -41,03 | | | [23] |
| Pacupahuain Cave | | Peru | P09 | | -11,24 | -75,82 | | | [26] |
| Pacupahuain Cave | | Peru | PH2 | | -11,24 | -75,82 | | | [26] |
| Paixão cave | | Brazil | PX7 | | -12,61 | -41,02 | | | [23] |
| Paixato cave | 113 | Brazil | PX7 | 228 | -12,62 | -41,02 | 14983 | 19144 | [24] |
| Palestina cave | 25 | Brazil | PAL3 | 93 | -5,92 | -77,35 | 22 | 851 | [27] |
| Palestina cave | 25 | Brazil | PAL4 | 94 | -5,92 | -77,35 | 100 | 1537 | [27] |
| Paraiso cave | 3 | Brazil | PAR01 | 20 | -4,07 | -55,45 | 714 | 4812 | [28] |
| Paraiso cave | 3 | Brazil | PAR03 | 21 | -4,07 | -55,45 | -48 | 768 | [28] |
| Paraiso cave | 3 | Brazil | PAR06 | 22 | -4,07 | -55,45 | 40683 | 44636 | [28] |
| Paraiso cave | 3 | Brazil | PAR07 | 23 | -4,07 | -55,45 | 17957 | 45144 | [28] |
| Paraiso cave | 3 | Brazil | PAR08 | 24 | -4,07 | -55,45 | 26490 | 28444 | [28] |
| Paraiso cave | 3 | Brazil | PAR16 | 25 | -4,07 | -55,45 | 4440 | 10927 | [28] |
| Paraiso cave | 3 | Brazil | PAR24 | 26 | -4,07 | -55,45 | 9476 | 28286 | [28] |
| Pau d'Alho cave | 52 | Brazil | ALHO6 | 128 | -15,21 | -56,8 | 90 | 1458 | [17] |
| Rainha cave | 111 | Brazil | RN1 | 219 | -5,6 | -37,73 | 4045 | 23890 | [8] |
| Rainha cave | 111 | Brazil | RN4 | 220 | -5,6 | -37,73 | 4393 | 17222 | [8] |
| Santana Cave | | Brazil | St-8 | | -24,53 | -48,73 | | | [29] |
| São Bernardo cave | | Brazil | SBE3 | | -13,81 | -46,35 | -60 | 827 | [21] |
| São Matheus cave | | Brazil | SMT5 | | -13,81 | -46,35 | 749 | 1686 | [21] |
| Shatuca cave | | Brazil | Sha-2 | | -5,7 | -77,9 | | | [30] |
| Shatuca cave | | Brazil | Sha-3 | | -5,7 | -77,9 | | | [30] |
| Tamboril cave | 27 | Brazil | TM0 | 97 | -16 | -47 | -32,22 | 1678 | [31] |
| Tamboril cave | 27 | Brazil | TM2 | 98 | -16 | -47 | 1485 | 3847 | [31] |
| Torrinha cave | 62 | Brazil | TR5 | 146 | -12,37 | -41,57 | -57 | 76 | [18] |
| Umajalanta | | Bolivia | Boto10 | | -18,12 | -65,77 | 604 | 1328 | [13] |

The onset of the monsoon season in tropical and subtropical South America begins in the austral Autumn (SON) as easterly trade winds associated with the southward shift of ITCZ, following maximum SSTs, and enhance moisture transport from the tropical Atlantic over the continent. Southward migration of insolation drives enhanced ocean-land heat gradient over the continent, leading to low-level convergence over the continent in turn increasing precipitation, and a

Preprints (www.preprints.org) | NOT PEER-REVIEWED | Posted: 5 October 2018 doi:10.20944/preprints201810.0094.v1

Peer-reviewed version available at Quaternary 2019, 2, 6; doi:10.3390/quat2010006

zone of deep convection is established at ~10 - 15°S over the southern Amazon Basin. This intense convection during the onset of the SAMS contributes to formation of an upper-level atmospheric high over Bolivia (Bolivian High; 15°S, 65°W), and a low-level atmospheric low over the Chaco region (Chaco low; ~25°S). This dynamic draws humid air from the core monsoon region, which is then transported south to the La Plata Basin region by the South American Low-Level Jet (SALLJ), because the easterlies at the core monsoon region are blocked by the Andes [2,32]. The monsoon reaches its mature phase in the austral summer (DJF) and the Bolivian High is well established. The South Atlantic Convection Zone (SACZ), a NW-SE trending band of convection that extends from the center of convection to the western South Atlantic, is a dominant feature of the mature SAMS (Figure 2). As a consequence of the establishment of the Bolivian High, divergent convection conditions occur in response to the increased upper level convergence, leading to subsidence and a deficit in summer precipitation over northeastern Brazil over the Nordeste (Nordeste Low) [33], which provides the antiphase relationship between the convection in the West and East of South America.

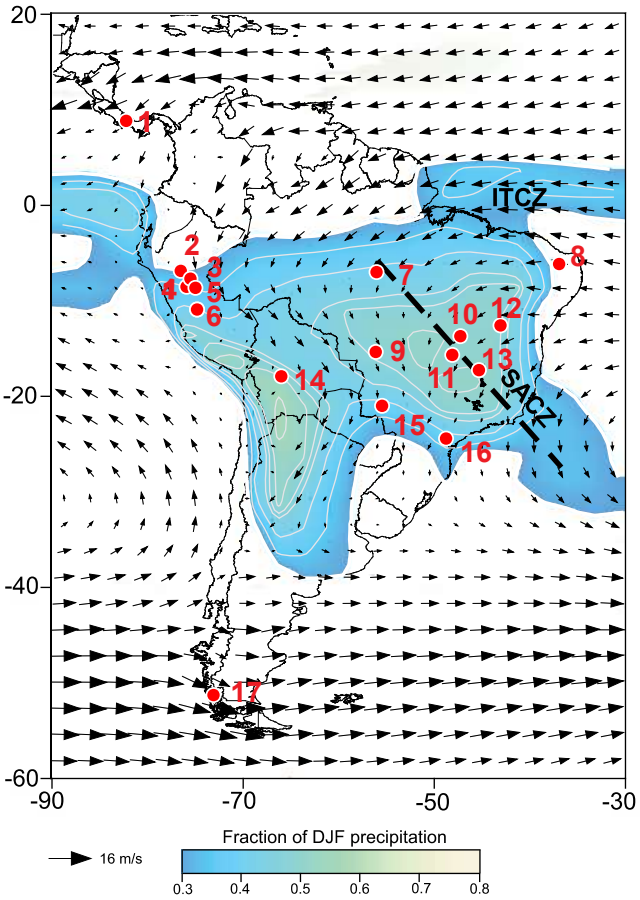


**Figure 2.** Map showing the core region of the South American Monsoon System (SAMS), the South American Convergence Zone (SACZ) and the Atlantic Intertropical Convergence Zone (ITCZ) (colour shading). Identified cave sites are indicated by closed red circles: 1) Chilibrillo cave; 2) Cueva del Diamante; 3) Tigre Perdido; 4) El Condor Cave; 5) Huagapo Cave; 6) Pacupahuain; 7) Paraiso Cave; 8) Rainha Cave, Abissal cave; 9) Pau d'Alho Cave and Curupira CaveAbissal cave; 10) São Bernardo and São Matheus Cave; 11) Tamboril Cave; 12) Diva Cave, Torrinha Cave, Lapa Doce Cave, Marota Gigante Cave and Paixão Cave; 13) Lapa Grande and Lapa Sem Fim; 14) Umajalanta Cave and Chiflonkhakha Cave; 15) Jaraguá Cave; 16) Botuverá Cave; 17) MA Cave. Also illustrated is the austral summer (December–February, DJF) 850 hPa wind field and fractional DJF precipitation. The core region of the SAMS is defined here for continental regions where the fraction of total annual

precipitation falling during austral summer (DJF) > 0.3; contour interval of the colour shading is 0.05. Wind data are from ERA-Interim [34] and precipitation data from GPCC [35], with averages calculated for the period from 1979 to 2014. Figure modified after ref [17].

In the following sections we first discuss aspects of all available (i.e. included in SISAL_v1) and identified speleothem records (Section 2). Section 3 presents results and discussion of past variation in the SAMS during the Late Pleistocene, the Holocene and the last 2 kyrs, utilizing speleothem $\delta^{18}O$ time series that are currently in SISAL_v1. However, we recognize the absence of critical records, and include, if necessary for the discussion, speleothem $\delta^{18}O$ time series that are not yet available in SISAL_v1. The Pleistocene section (Section 3.1) sets the focus on variations of the SAMS that are associated with changes in insolation due to variations in Earth's orbit and millennial scale variations. The Holocene section (3.2) details discrepancies and similarities between speleothem $\delta^{18}O$ time-series and potential drivers of these variations. The last section (3.3) focuses on hydroclimate scenarios of the last two millennia, such as the Little Ice Age (LIA), the Medieval Climate Anomaly (MCA) and the Current Warm Period (CWP), and further, identifies the possible climate drivers of the SAMS and ITCZ during this period.

## 2. Assessing SISAL_v1 for South America

Thus far 75 individual specimen (speleothem isotope time series) from South America have been identified (Table 1). From these identified 75 speleothem isotope time series 31 are already available in SISAL_v1 whereas the remaining 44 (not including isotope time series that are not published yet) will be added to the SISAL database in the near future. Currently, almost all isotope time series in SISAL_v1 are in the domain of the South American Monsoon System (SAMS) (Figure 1 and 2). However, many speleothem isotope time series that are identified but not included yet, are also located within the zone of influence of the SAMS (Figure 1 and 2) – only the records from Patagonia (MA cave) and Panama (Chilibrillo cave) are not influenced by the SAMS. Therefore, SISAL_v1 and future updates of the SISAL database are especially suitable to investigate spatio-temporal variations of the SAMS.

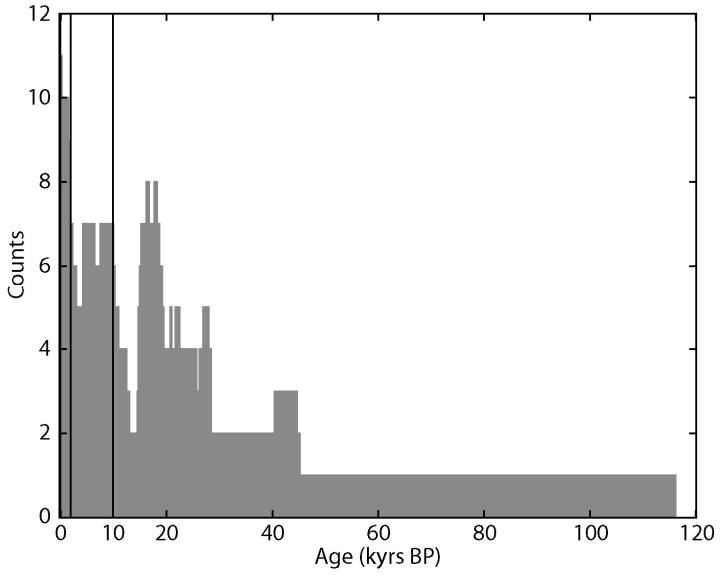


**Figure 3.** Histogram of SISAL_v1 speleothem isotope time series during the last 120 kyrs from South America. For this the 120 kyrs time window was subdivided in 250-year long bins and available speleothem isotope time series were counted if at least one $\delta^{18}O$ value was within a bin. The two vertical boxes indicate the last 10 kyrs and 2 kyrs, respectively.

The SISAL_v1 $\delta^{18}O$ time series cover more or less the last 120 kyrs (Figure 3). However, the distribution of speleothems $\delta^{18}O$ time series is clearly biased towards the last 30 kyrs. In the time from 120 kyrs BP to about 50 kyrs BP, only one $\delta^{18}O$ time series is available (BT2 from Botuverá cave). In the time from 30 kyrs BP to present day, the most $\delta^{18}O$ time series are available for the last 2 kyrs followed by the Holocene and the LGM. This non-uniform temporal distribution of $\delta^{18}O$ time series is explained mainly by the focus of the research articles that published the $\delta^{18}O$ time series. Thus, Figure 3 indicates that speleothem $\delta^{18}O$ time series in SISAL_v1 are especially suitable for analyses of past variations in the SAMS in the period from 30 kyrs BP to present day. Applications of the SISAL for analysis of the SAMS are further elaborated in Section 4.

## 3. Results and Discussion

### *3.1. Pleistocene variations of the SAMS as recorded by speleothem $\delta^{18}O$ time series*

This section is subdivided into two parts discussing, i) speleothem $\delta^{18}O$ time series that show orbital scale changes and, ii) speleothem $\delta^{18}O$ time series exhibiting millennial-scale climate changes.

#### 3.1.1. Insolation forced changes of the SAMS

Thus far only a few published speleothem $\delta^{18}O$ time series show orbital scale changes. These include stalagmites BT2 [6], BTV4A*, BTV4C* [11] from Botuverá cave, St8* [29] from Santana cave, which are all located in southeastern Brazil. (An asterisk indicates entities that are not included in SISAL_v1.) Furthermore, speleothem $\delta^{18}O$ time series from El Condor (ELC*) and Cueva del Diamante (NAR*), located on the eastern side of the Andes (northern Peru) and western Amazonia, respectively, show pronounced orbital scale changes [15] (Figure 1). We note that such orbital-scale changes are not observed in eastern Amazonia during the last 40 kyrs [28]. In the following, the focus is only on speleothem $\delta^{18}O$ time series of Botuverá (BT2) and from western Amazonia.

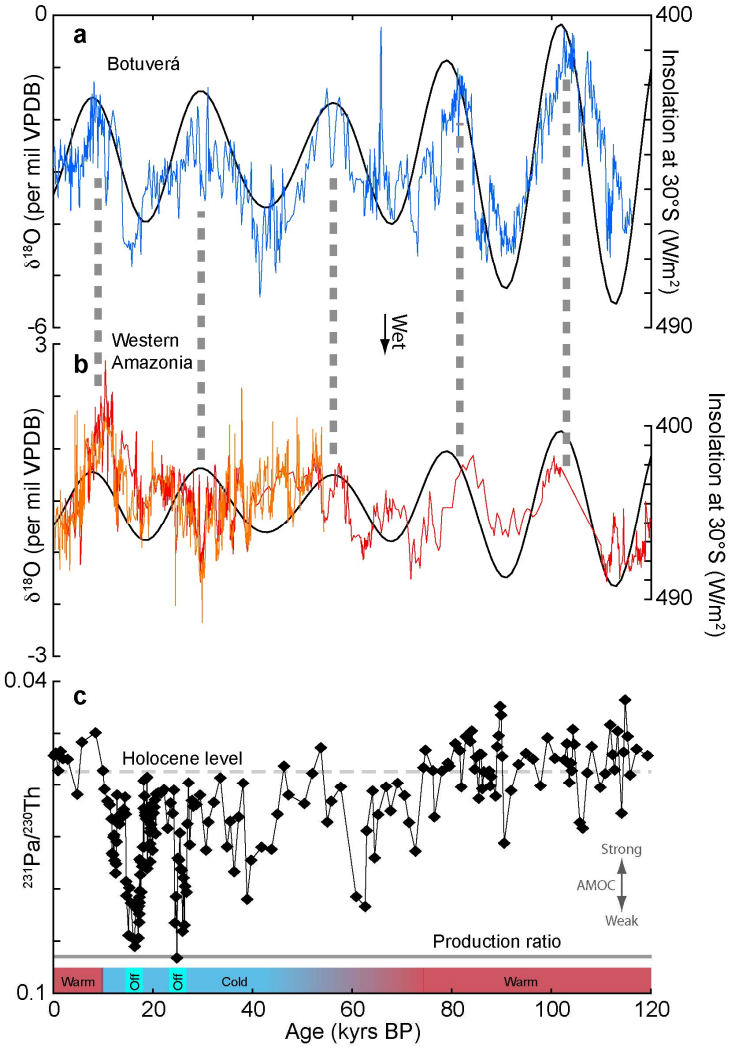


**Figure 4.** Orbital scale changes in South American speleothems inferring insolation driven changes of the SAMS. (**a**) Speleothem $\delta^{18}O$ time series of BT2, Botuverá cave (southeastern Brazil) [6] and the austral summer insolation in February at 30°S. (**b**) Speleothem $\delta^{18}O$ time series from El Condor (red) and Cueva del Diamante (orange), Western Amazonia [15] and the austral summer insolation in February at 30°S [36]. Note that the shown speleothem $\delta^{18}O$ are composed of several individual speleothems and are set to a mean $\delta^{18}O$ value of 0 (see text for detail). Speleothem $\delta^{18}O$ values indicate wetter conditions if $\delta^{18}O$ values are decreasing. Vertical dashed lines indicate maxima of the BT2 $\delta^{18}O$ time series. (**c**) $^{231}Pa/^{230}Th$ time series from ODP site 1063 which infers variations in the strength of the Atlantic Overturning Circulation (AMOC) [37]. A decreasing $^{231}Pa/^{230}Th$ ratio indicates an increase of the strength of the AMOC while decreasing $^{231}Pa/^{230}Th$ ratio point towards a slowing down of the vigour of the AMOC. If the $^{231}Pa/^{230}Th$ ratio is close to or reaches the production ratio the AMOC is in its off mode. This $^{231}Pa/^{230}Th$ time series indicates that AMOC is in its warm mode (strong AMOC) until about 70 kyrs when it begins to weaken until the LGM where two pronounced stops of the AMOC are recognised associated with Heinrich Stadial 1 and 2, respectively (light blue bars at bottom of the figure). During the Holocene the AMOC is again in its warm mode. See Böhm et al. [37] for details.

BT2 grew continuously during the last c. 112 kyrs and the $\delta^{18}O$ time series exhibits pronounced orbital scale changes that follow the austral summer insolation (Figure 4a) [6]. Changes in BT2 $\delta^{18}O$ values are determined by the varying contribution of moisture that originates from the Amazon basin that is associated with monsoonal rainfall (low $\delta^{18}O$) during summer and the adjacent South

Atlantic ocean (high $\delta^{18}O$) in winter [6,7]. Therefore, changes in BT2 $\delta^{18}O$ reflect mainly the varying contribution of monsoonal rainfall to the annual rainfall in southeastern Brazil caused by shifts of the SACZ [8]. These shifts are possibly caused by latitudinal shifts of the termini of the Hadley cell (i.e. the width) or by the rainfall history of the moisture that is transported from the Amazon basin towards southeastern Brazil by the SALLJ [6].

Combined, the stalagmite $\delta^{18}O$ time series from El Condor (ELC-A*, ELC-B*) and Cueva del Diamante (NAR-C*, NAR-D*, NAR-F*) cover more or less the last 250 kyrs [15]. However, since BT2 covers the last 112 kyrs only, the following discussion is limited to this period. In the following the combined stalagmite $\delta^{18}O$ time series from El Condor and Cueva del Diamante is stated as the western Amazonia (WA) $\delta^{18}O$ time series. $\delta^{18}O$ values in the WA speleothem $\delta^{18}O$ time series are primarily controlled by the amount effect related to SAMS rainfall in summer as well as the rainfall history and the moisture-recycling by transpiration over the Amazon basin; which may attenuate the true rainfall history, because transpiration is a non-fractionation process [15]. The WA $\delta^{18}O$ time series follows, with some exceptions, the austral summer insolation, though less perfect compared to BT2 and is therefore also broadly in-phase with the BT2 $\delta^{18}O$ time series (Figure 4 a,b). Marked differences between the $\delta^{18}O$ time series from Botuverá and western Amazonia occur in the period from 50 kyrs BP to 20 kyrs BP when the two time series appear to be anti-correlated. Thus, when $\delta^{18}O$ time series of BT2 decreases, indicating wetter conditions in southeastern Brazil, $\delta^{18}O$ values in the WA speleothems increase, inferring dryer conditions in western Amazonia. This change in the phase-relationship between BT2 and the WA speleothems is also observed between the WA $\delta^{18}O$ time series and the austral summer insolation (Figure 4b). The WA $\delta^{18}O$ time series appears to be out-of-phase with the austral summer insolation in the period from c. 60 kyrs BP to 20 kyrs BP. This feature is further elaborated below. The coherence of the orbital scale changes between the speleothem $\delta^{18}O$ time series from southeastern Brazil and western Amazonia in the period until c. 60 kyrs BP and from 20 kyrs BP to present-day indicates that SAM rainfall broadly co-varies in these distant regions and appears to be mainly controlled by changes in the austral summer insolation forced by variations in Earth's precession whereas increasing austral summer insolation provokes an intensification of the South American Monsoon System [6,15]. The proposed mechanism beyond this insolation forcing of the SAMS is that increasing insolation causes stronger continental heating which in turn provokes a stronger convective activity. This increases the convective heating and vertical updraft in the core monsoon region. It provokes also an intensification of the Nordeste Low and increases subsidence in northeast Brazil, respectively, resulting in generally arid conditions in this region (higher $\delta^{18}O$ values) [8,15].

The WA $\delta^{18}O$ time series appears to be in-phase with the austral summer insolation (i.e. degreasing $\delta^{18}O$ values correlate with increasing summer insolation) until c. 60 kyr BP and the last 20 kyrs and is out-of-phase in the period from 60 kyr BP to 20 kyr BP (see above). Interestingly, the period when the WA $\delta^{18}O$ time series is out-of-phase with the austral summer insolation, the strength of the Atlantic Meridional Ocean Circulation (AMOC) is reducing and switches in its glacial (cold) mode [37] (Figure 4c). This infers that the oceanic meridional heat transport is reduced in this period, which should, according to energetic constrains, force a southward migration of the ITCZ [38,39]. This possibly alters rainfall pattern associated with the SAMS especially at the northern side of the core monsoon region in the Amazon basin and western Amazonia, respectively. Hence, the WA stalagmites are possibly located in a strategic location where rainfall responds differently to the austral summer insolation depending on the strength of the AMOC and inter-hemispheric temperature contrasts, respectively. Hence, when the AMOC is in its cold mode, the ITCZ and the core monsoon region shifts poleward and Western Amazonia is located at the boundary of core monsoon region. Rainfall in western Amazonia depends then mainly on spatial shifts of the precipitation pattern associated with the SAMS and not on the rainfall amount. If the austral summer insolation increases in such a case the ITCZ and the core monsoon region may be shifted even further south due to a warmer Southern Hemisphere in turn provoking decreasing precipitation amounts in western Amazonia (i.e. increasing $\delta^{18}O$ values in WA speleothems). In contrast, this causes increasing precipitation amounts when the austral summer insolation decreases

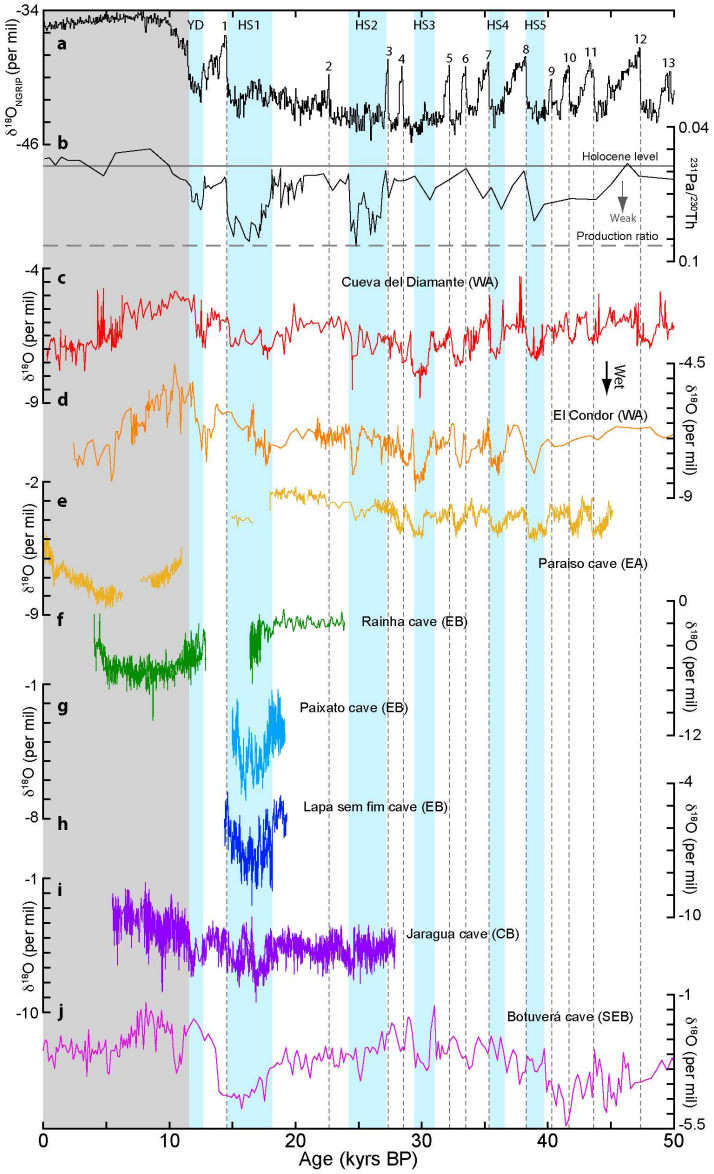


because the ITCZ and the core monsoon region shifts equatorwards provoking decreasing $\delta^{18}O$ values in WA speleothems.

3.1.2. Millennial-scale climate events

Millennial scale climate variability associated with Dansgaard-Oeschger and Heinrich stadials in the Northern Hemisphere are observed all across the region that is under influence of the SAMS. The region that is most sensitive to these Northern Hemisphere climate modes is northeastern Brazil (Nordeste) where semi-arid conditions prevail at present. However, speleothem and travertine growth periods during the last 220 kyrs reveal that during Heinrich stadials rainfall amounts increase substantially in this region allowing for speleothem and travertine growth [40]. Increasing rainfall amounts during Heinrich stadials are also inferred by changes in speleothem $\delta^{18}O$ values observed in Central (Lapa Sem Fim Cave: LSF3, LSF9*, LSF11*, LSF13*, LSF15*, LSF16; Lapa Grande: LG3, LG10*, LG11, LG12B*, LG25*) and northeast Brazil (Paixão Cave, PX5*, PX7; Marota: MAG*) [23,24], middle-western Brazil (Jaraguá Cave: JAR7, JAR14, JAR13) [20] as well as in eastern (Paraiso cave: PAR01, PAR03, PAR06, PAR07, PAR08, PAR16, PAR24) [28] and western Amazonia (El Condor: ELC-A*, ELC-B*; Cueva del Diamante: NAR-C*, NAR-D*, NAR-F*) [15] and southeastern Brazil (Botuverá cave: BT2, BTV3A*, BTV4A*, BTV4C*) [6,10,11] (Figure 5).

**Figure 5.** Millennial-scale changes in South American speleothems during the last 50 kyrs reveal coherent changes in rainfall associated with variations in the SAMS activity. (**a**) North GRIP $\delta^{18}O$ time series showing millennial scale climate changes associated with Dansgaard-Oeschger (DO) stadials [41]. DOs are numbered beginning with 1 and are increasing with time and the beginning of each DO is indicated by a vertical dashed line. (**b**) $^{231}Pa/^{230}Th$ time series from ODP site 1063 (see also Figure 4), which infers variations in the strength of the Atlantic Overturning Circulation (AMOC) [37]. This $^{231}Pa/^{230}Th$-based reconstructions of the vigour of the AMOC shows that the AMOC-strength is greatly reduced during Heinrich stadials (HS) (blue shaded bars), especially during HS1 and HS2, when the AMOC is in its off mode. Western Amazonia (WA) speleothem $\delta^{18}O$ time series include speleothems from (**c**) Cueva del Diamante (NAR-C*, NAR-D*, NAR-F*) and (**d**) El Condor (ELC-A*, ELC-B*) [15]. (**e**) Speleothem $\delta^{18}O$ time series from Eastern Amazonia are from Paraiso cave (PAR01, PAR03, PAR06, PAR07, PAR08, PAR16, PAR24) [28]. Speleothem $\delta^{18}O$ time series from Eastern Brazil (EB) are from (**f**) Rainha cave (RN1, RN4) [8], (**g**) Paixão Cave (PX7), (**f**) Lapa sem fin cave (LSF3, LSF16) [24]. (**h**) Jaraguá Cave (JAR7, JAR14, JAR13) is located in mid-western (central) Brazil (CB) [20] while (**i**) Botuverá cave (BT2) is located in southeastern Brazil (SEB) [6].

The coherent response of rainfall increases all across the regions under SAMS influence during HS1 is termed as the Mega-SACZ [24]. The comparison of the South American SISAL_v1 $\delta^{18}O$ time series together with the $\delta^{18}O$ time series from Western Amazonia (Figure 5) and new findings from northeastern Brazil [23] that are yet to be included in the SISAL database, show an increase of rainfall during Heinrich stadials during the last 50 kyrs. These responses in rainfall amounts across the SAMS domain suggests that the development of a Mega-SACZ is not only restricted to HS1 but to Heinrich stadials in general since the Emian. The speleothem and travertine growth periods from northeastern Brazil, which date back 220 kyrs, hint that this could have been also the case before the Emian [40]. However, this is only a hypotheses and certaintly requires the generation of new high-resolution speleothem $\delta^{18}O$ time series from all across the SAMS region. The suggested mechanim for the development of the Mega-SACZ is a strengthening of the cross-equatoral heat transport related to changes in Sea Surface Temperatures (SSTs) in the tropical Atlantic [24]. This would be consistent with results of modelling experiments investigating the effect of a mid-latitude Northern Hemisphere cooling through an AMOC shutdown, which provokes a change in SSTs in the tropical Atlantic [42]. However, in this study, drier conditions would occur in northeast Brazil, which contradics to some extent the speleothem-based rainfall reconstructions. It is not clear at this stage why the modelling and the empirical results show opposite trends in response to Heinrich stadials (NH cooling); further work is necessary to work out the discrepancies. It may also highlight Nordeste as a key region for data-model comparisons.

### *3.2 Holocene variations of the SAMS as recorded by speleothem $\delta^{18}O$ time series*

We note that many published records partially cover the Holocene. However, very few of these records are currently included in the SISAL database (SISAL_v1), and even fewer of these records cover the entire extent of the Holocene (Table 1). In this review we only include speleothem $\delta^{18}O$ time series that cover the Holocene (i.e., early-, mid-, and late- subdivisions) to assure the ability to discuss dynamics related to the Holocene climate variability of the SAMS (Figure 6). These records include PAR01, PAR03, and PAR16 [28] from Paraíso Cave, LG3 and LG11 [22] from Lapa Grande Cave, and BT2 [6] and BTV21a [9] from Botuverá Cave. These caves are from the eastern Amazon, central Brazil, and southeast Brazil. While not included in SISAL_v1 yet, we note that several speleothem $\delta^{18}O$ time series from the Western Amazon and Peruvian Andes are similar to the Botuverá record from SE Brazil in the context of Holocene rainfall changes (Figure 5) inferring also increasing precipitation amounts during the Holceoen. Thus, discussion of the Botuverá cave records may, but not certainly, apply to those sites.

In South America, the Holocene is characterized by increasing austral insolation through the entire Holocene. This insolation trend is matched by the Botuverá $\delta^{18}O$ records (Figure 6), but is notably absent in speleothem $\delta^{18}O$ time series from Paraíso cave (eastern Amazon) and Lapa Grande

Preprints (www.preprints.org) | NOT PEER-REVIEWED | Posted: 5 October 2018 doi:10.20944/preprints201810.0094.v1

Peer-reviewed version available at Quaternary 2019, 2, 6; doi:10.3390/quat2010006

(central Brazil). Instead, the Lapa Grande $\delta^{18}O$ time series exhibits a relatively stable trend, while Paraiso tracks insolation from the early- to mid-Holocene, and then diverges from the mid-Holocene (~8 ka) to present. Globally, the Holocene is often cited as a period of stable climate, relative to previous periods, as evidenced from little variance in Greenland and Antarctica ice core records [43,44] (Fig. 4a). Periods of abrupt climate change in the Holocene, such as the 8.2 kyr event and Bond events [45], are superimposed on this stable climate. Further, regional climatic anomalies are emerging in the literature, including The Holocene Climatic Optimum and the 4.2 kyr event [46,47]. How these events are manifested, and if at all, in tropical and subtropical South America remains uncertain. Climatic anomalies constrained to the last 2-kyr will be discussed in Section 2.3, and are not detailed here.

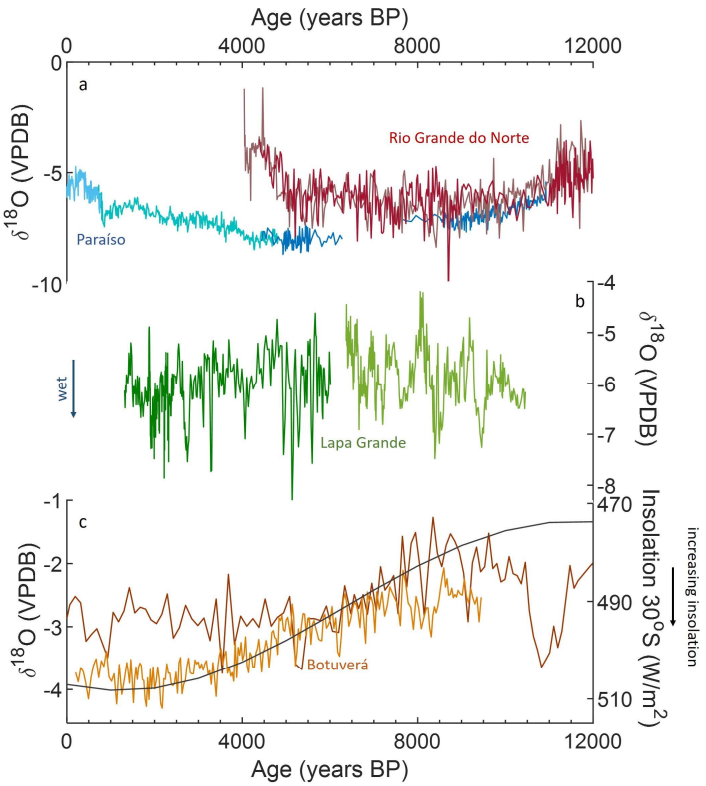


**Figure 6.** Holocene speleothem $\delta^{18}O$ time series available in SISAL_V1. (a) Paraíso Cave (blue) (PAR01, PAR03, and PAR16) and Rio Grande do Norte (red) (RN-1 and RN-4), (b) Lapa Grande (LG3 and LG11), and (c) Botuverá (BT-2 and BTV21a).

*3.2.1 Insolation Driven Holocene $\delta^{18}O$ records*

As previously discussed in Section 2, detailing Pleistocene records, the proposed mechanism driving the Botuverá $\delta^{18}O$ time series is intensification of the SAMS as driven by increasing summertime insolation. Therefore, a progressive increase of the precipitation amount trough the Holocene period is inferred from the Botuverá $\delta^{18}O$ time series. We note that this does not necessarily suggest that precipitation amount increased in SE Brazil coupled with increasing monsoon intensity, but rather that SE Brazil received more $\delta^{18}O$-depleted precipitation from increased convection upstream, within the core of convection in the monsoon region [5]. That is, increased convection within the core monsoon region leads to more depleted water masses, which then lead to depleted precipitation along the entire water mass trajectory, relative to periods of weakened monsoon convection. Thus, it might be expected that any regions along the monsoon

trajectory will exhibit the same $\delta^{18}O$ values, unless mechanisms beyond monsoon intensity are driving these records [5]. Such mechanisms may be increased (decreased) local precipitation or changes in relative contributions of water-mass sources (e.g. [8]). However, a speleothem Sr/Ca time series from Botuverá cave, a proxy for the local effective rainfall [48], clearly shows that rainfall amounts increase in this region with increasing influence of SAMS rainfall during the course of the Holocene [9]. Therefore, other speleothem measurements, such as trace elements, can yield important complementing information to $\delta^{18}O$ values and shed further light on past monsoon variability. While not available in the SISAL_v1 yet, speleothem $\delta^{18}O$ records from the Peruvian Andes, El Condor and Cueva Diamante records (as previously discussed) as well as Haupago Cave [19] and lake and ice core records [49] all exhibit $\delta^{18}O$ values that follow Botuverá Cave and insolation, suggesting these sites along the monsoon water-mass trajectory are being influenced by increased monsoon convection and/or increases in local precipitation amount potentially due to increased water availability associated with increased monsoon strength.

*3.2.2 Dipole of Holocene $\delta^{18}O$ values*

The South American rainfall dipole inferred by $\delta^{18}O$ values of NE Brazil (Nordeste) and the rest of the monsoon domain on orbital timescales seems to be also persistent during the Holocene. Although the Rio Grande do Norte (RN-1 and RN-4) $\delta^{18}O$ records of the SISAL database do not cover the entirety of the Holocene, they are discussed here for their pertinence to discussion of the observed climatic dipole. Notably, the RN records are in-phase with the Paraiso $\delta^{18}O$ time series (eastern Amazon) for the length of the RN records, although the increasing $\delta^{18}O$ values of the RN records in the mid-Holocene are more pronounced compared to the Paraiso $\delta^{18}O$ time series (Figure 6). The proposed rainfall dipole between the Nordeste and the rest of the SAMS domain is not readily apparent in the early-Holocene (~12 – 8 ka) $\delta^{18}O$ time series available here, but becomes distinct in the time from the mid- to late-Holocene between the RN and Paraiso $\delta^{18}O$ time series and the Botuverá $\delta^{18}O$ time series (Figure 6).

*3.2.3 Holocene Variations of the SACZ*

The stable trend of $\delta^{18}O$ values at Lapa Grande cave is unique among the speleothem $\delta^{18}O$ time series available in the SISAL_v1, particularly over longer time scales (Figure 6). One possible driver of the variability in the Lapa Grande $\delta^{18}O$ time series are changes in regional rainfall amounts associated with latitudinal fluctuations of the SACZ (Figure 2). This is further elaborated in Section 2.3. In short, latitudinal fluctuations and shifts of the SACZ affect rainfall amounts in proximal regions while precipitation amounts in the center of the SACZ are possibly very constant [21]. Thus, Lapa Grande's position within the center of the SACZ, and steady mean $\delta^{18}O$ values of Lapa Grande speleothems during the Holocene, imply little change in precipitation amount at this site, possibly because it was under the influence of the SACZ during the entire Holocene. This would suggest the Lapa Grande Cave $\delta^{18}O$ time series are not dominantly influenced by upstream rainout in the core monsoon region, but rather local rainfall amount associated with the strength of the SACZ. If so, this suggests the SACZ has not increased or decreased in intensity throughout the entirety of the Holocene, despite increasing insolation and increasing intensity in the core of monsoon convection in the Amazon Basin. Stríkis et al. (2011) [22] identify depleted $\delta^{18}O$ episodes in the Lapa Grande record that coincide with the cold Bond events in the Northern Hemisphere. It was interpreted by the authors as a result of the southward positioning of the ITCZ following the same mechanism, but with smaller amplitude, as occurred during the Heinrichs stadials in the South America. The abrupt climate events that occurred at 2.7 ka and 8.1 ka were also documented in speleothems in the Northeast Brazil [18,50].

*3.3 Variations of the SAMS during the last 2 kyrs as recorded by speleothem $\delta^{18}O$ time series*

Peer-reviewed version available at Quaternary 2019, 2, 6; doi:10.3390/quat2010006

For the last two millennia 10 stalagmite records from 6 different regions are in the current SISAL database. Most of the presented records only have the $\delta^{18}O$ data available, their resolution is approximately annual and, with exception of the ALHO6 stalagmite that is annually laminated, all speleothems age models are based on U/Th ages. These stalagmites are from Northeast Brazil [18], Southeast Brazil [5], Central Brazil [21,31], middle-western Brazil [17,21], Amazon [28], Peruvian Andes [12,27,30] and Bolivian Andes [13].

The main climate features during the last two millennia in South America was determined by the warm and could periods in the Northern Hemisphere (NH) during the Medieval Climate Anomaly (MCA) and the Little Ice Age (LIA), respectively [5,49]. Warm conditions in the NH determines a northward positioning of the ITCZ what depletes the moisture of the SASM. It was documented during the MCA period in speleothem records from Diva Cave from Northeast Brazil [18], Pau d'Alho and Jaraguá caves from mid-western Brazil [17,21], Palestina [27] and Cascayunga caves [12] from the Peruvian Andes. However, speleothem records from Tamboril [31] and São Bernardo [21] caves located in central Brazil, and Crystal cave [5] from southeast Brazil do not show a significant anomaly at this period. Intriguing, speleothem record from the Umajalanta–Chiflonkhakha cave system in the eastern Bolivian Andes [13] show increase of the convective activity during the MCA period, which was interpreted by the authors as a result of a different mechanism (not ITCZ/SAMS system), which implies that was moisture sourced mainly from the southern tropical Atlantic.

The southward positioning of the ITCZ during LIA period was responsible for the wet conditions documented in the majority of the speleothem records in the South American [21], as for example, was documented in the caves: Pau d'Alho (Novello et al., 2016), Jaraguá [21], Palestina [27], Cascayunga [12] and Crystal [5]. However, during this period, the SACZ (an internal feature of SAMS responsibly by its variability) was also displaced southward what provided an antiphase of convection between southwest and northeast portions of the SAMS domain [21]. Thus, while records from southwest of SAMS domain show wet conditions [5,12,13,17,21,27] the records from northeast represented manly by the Diva cave [18] show dry conditions. As a consequence, the records located near the node of this dipole (São Matheus and Tamboril caves), which experienced continuous SACZ influence at all times, hence displaying neutral moisture conditions during the LIA period and no trend over the last millennium (Figure 7) [21].

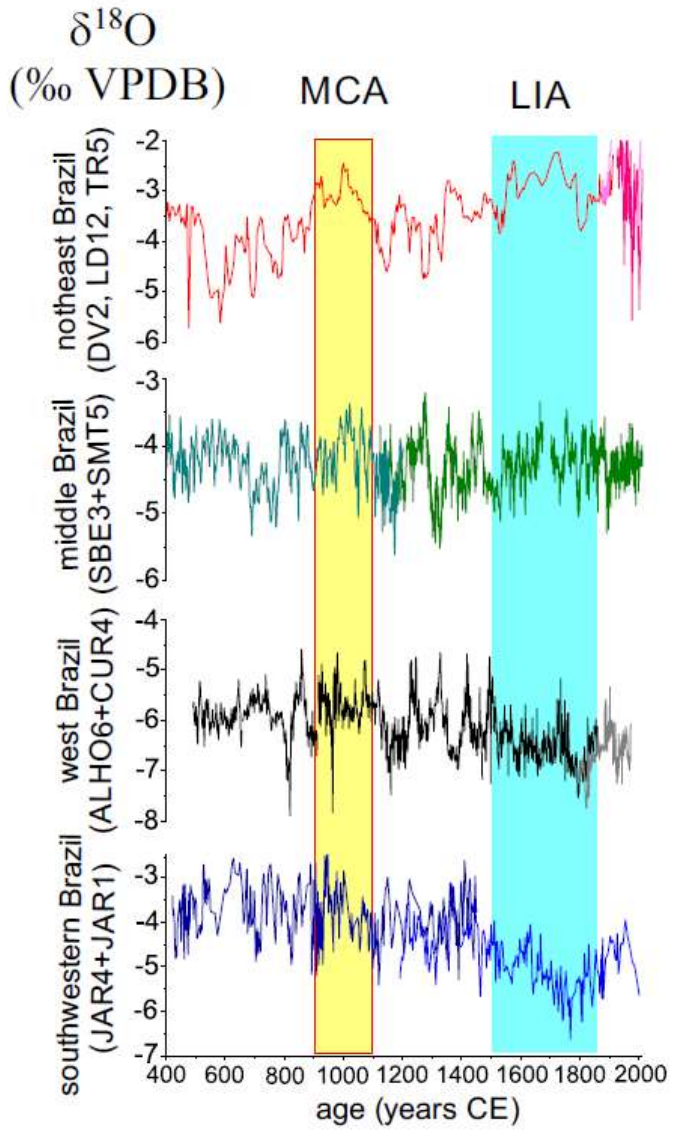


**Figure 7.** Holocene speleothem $\delta^{18}O$ time series for the last 2kyrs: northeast Brazil (DV2 stalagmite – Diva Cave, TR5 stalagmite – Torrinha cave, LD12 – Lapa Doce); middle Brazil (SBE3 stalagmite – São Bernardo Cave, SMT5 stalagmite – São Matheus Cave); middle Brazil (ALHO6 stalagmite – Pau d'Alho Cave, CUR4 – Curupira Cave), and southwestern Brazil (JAR4 and JAR1 stalagmites – Jaraguá Cave). Figure modified from Novello et al. (2018).

During the Current Warm Period (CWP), after the LIA, the convective conditions over South America appears to be similar to the MCA, which means, warming in the NH, a northward positioning of ITCZ and a progressive weakening of the SAMS.

A centennial periodicity of the SAMS (around 210 years) was reported from different sites [17,18,27] and is associated with the de Vriess-Suess solar cycle, with depleted $\delta^{18}O$ during high solar irradiance periods. It is suggested that this relationship is due to several feedbacks involving amplification of solar forcing by coupled air-sea dynamics, cloud formation and stratospheric warming due to enhanced UV absorption through increased stratospheric ozone concentration, resulting adjustment in the Hadley cell modulates the position of the ITCZ and SACZ (Novello et al., 2016 and references therein) [17]. Multidecadal variability (60 – 90 years) associated with the Atlantic

Multidecadal Oscillation (AMO) also affect the SAMS, with a more southerly position of the ITCZ during its negative phase (warm in southern tropical Atlantic) Cruz

[17,18,27]. Although El Niño–Southern Oscillation (ENSO) may be a predominant forcing over the SAMS in the current climatology, there is no exist evidence of the influence of this mode into the past millennia. The argument against an ENSO influence at the time is related to the often synchronous climate conditions observed between the Peruvian Andes and southeast Brazil during the last two millennia, even though the canonical ENSO impact in these two regions is the exact opposite [5,21].

## 4. Conclusion and Outlook

### *4.1 Summary on SAMS variability*

The speleothems $\delta^{18}O$ time series from South America are interpreted mainly as proxies of amount effect and infer past variations of the Intertropical Convergence Zone (ITCZ), the South America Monsoon System (SAMS) and of the South Atlantic Convergence Zone (SACZ). Precession driven insolation is the main driver of convective variability over the continent during the last 250 kyrs, including the Holocene period. A climate dipole is observed between the west and east portions of the continent, which is most prominent on orbital time scales. Records located in the central region of Brazil appear to be weakly affected by insolation and are more susceptible to the variations of the SACZ. Cold episodic events in the Northern Hemisphere are responsible for the southward position of the ITCZ and increases rainfall in the SAMS domain on all times scales, as were documented during millennial events from the last glacial period (Heinrich events), Bond events during the Holocene, as well as during the Little Ice Age. Variations in Northern Hemisphere temperatures were the main forcing of changes in SAMS during the last two millennia, which resulted in a predominant dry condition during the Medieval Climate Anomaly and wet conditions during the LIA, which was followed by progressive arid condition during the Common Warm Period.

### *4.2 Outlook and potentials for future speleothem-based empirical research*

Most speleothem records from South America are located in the tropical region of the Southern Hemisphere. Many of these speleothems are from high altitudes sides in the Andes, which are under influence of the SAMS. Thus far, no records are available from north of the equator and only one record was documented from the high latitudes of South America (Figure 1 and 2). The next challenge for a better understanding of past changes in the South American hydroclimate will be through the generation of new speleothem proxy time series that are located outside of the SAMS domain. Furthermore, another step for a deeper understanding of the South American hydroclimate and the SAMS in particular is the generation of longer time series. Most of the studies conducted so far are not longer than 50 kyrs, and only a few time series are longer than 100 kyrs (Figure 3). In addition to $\delta^{18}O$, complementing speleothem proxies should be measured, such as trace elements or elemental isotope ratios (e.g. $^{87}Sr/^{86}Sr$), to explore the relationship between local precipitation and regional monsoon strength [9,31]. Furthermore, speleothem $\delta^{13}C$ records, which are usually neglected in the many studies related to monsoon reconstructions can be used for reconstructions of the palaeovegetation or soil dynamics [51,52].

### *4.3 Next steps and potentials for SISAL-based research*

Critically for SISAL-based research is that identified and not included speleothem isotope time series need to be added to the SISAL database in the near future (Table 1). This will greatly improve the spatio-temporal coverage of the SAMS domain (Figure 1 and 2), in turn allowing to perform detailed analysis of past variations of the SAMS using the SISAL database. Such analysis should not only be focused on speleothem $\delta^{18}O$ time series but also on the available $\delta^{13}C$ time series. This is of particular interest, because $\delta^{13}C$ is in most cases not discussed, but yields additional insights in the response of the palaeovegetation on variations of the SAMS. Better understanding of such SAMS-vegetation feedbacks are not only important for a better understanding of spatio-temporal

$\delta^{18}O$ variations (moisture recycling) [28] but also to better predict the response of the tropical rain forest to precipitation changes in the Amazon basin (an important carbon sink or source) in response to global warming. By using $\delta^{18}O$ as a proxy for past precipitation variations, speleothem $\delta^{18}O$ time series in the SISAL database are very appropriate for data-model comparisons. This does not necessarily include only isotope enabled climate models, because trends in speleothem $\delta^{18}O$ time series – and patterns – yield also information on whether specific regions got wetter or drier in the past, which is in many cases already sufficient to test the response of a climate model to e.g. NH cooling. Such a test case for data-model comparisons are Heinrich stadials or the transition from the early to the late Holocene where on the one hand many records are available (e.g. Heinrich stadial 1) and on the other hand changes in the hydroclimate were so pronounced that a comparison of trends in isotope and non-isotope climate models is possible. A strategic region for such tests is northeastern Brazil (Nordeste), which is at present dominated by semi-arid conditions, but was much wetter during Heinrich stadials or in the mid-Holocene [8,40]. Hence, comparison with climate models is essentially easy for this region. Considering that variations of precipitation in northeastern Brazil are linked to the low-level circulation of the SAMS, which appears to be even linked to the tropical atmospheric circulation in Africa [8], accurate modeling of the precipitation in Nordeste is a crucial benchmark test for the tropical atmospheric circulation in climate models. Furthermore, to get a deeper understanding of spatio-temporal changes of past changes of the SAMS, the SISAL database can be used to perform spatio-temporal analysis using e.g. MC-PCA techniques [53]. This could help to better constrain the different forcing and coherence of precipitation changes in the core monsoon region (central Brazil) and regions that are mainly influenced by shifts of the SACZ (southeastern Brazil). Such analysis could be also used for a better understanding of the drivers of variations in $\delta^{18}O$ time series, if these are caused by local amount effects or dominated by downstream processes associated with the precipitation history and recycling of moisture [5,15,28]. In summary, the SISAL database makes it possible to conduct a variety of different analysis of the South American Monsoon System, which will ultimately yield to a better understanding of its past changes.

**Author Contributions:** All authors contributed equally to this manuscript.

**Funding:** MD acknowledges funding by the German Research Foundation (DFG) grant DE 2398/3-1.

**Acknowledgments:** SISAL is a working group of the Past Global Changes (PAGES) programme and we thank PAGES for their support of this activity. We thank to Laia Comas Bru for comments, which helped to improve the manuscript and for editorial handling of the manuscript. We thank the World Karst Aquifer Mapping project (WOKAM) team for providing us with the karst region map presented in Figure 1

**Conflicts of Interest:** The authors declare no conflict of interest.

## References

1. Schneider, T.; Bischoff, T.; Haug, G.H. Migrations and dynamics of the intertropical convergence zone. *Nature* **2014**, *513*, 45-53.
2. Vera, C.; Higgins, W.; Amador, J.; Ambrizzi, T.; Garreaud, R.; Gochis, D.; Gutzler, D.; Lettenmaier, D.; Marengo, J.; Mechoso, C.R., et al. Toward a Unified View of the American Monsoon Systems. *Journal of Climate* **2006**, *19*, 4977-5000, doi:10.1175/JCLI3896.1.
3. Atsawawaranunt, K.; Comas-Bru, L.; Amirnezhad Mozhdehi, S.; Deininger, M.; Harrison, S.P.; Baker, A.; Boyd, M.; Kaushal, N.; Ahmad, S.M.; Ait Brahim, Y., et al. The SISAL database: a global resource to document oxygen and carbon isotope records from speleothems. *Earth Syst. Sci. Data* **2018**, *10*, 1687-1713, doi:10.5194/essd-10-1687-2018.
4. Chen, Z.; Auler, A.S.; Bakalowicz, M.; Drew, D.; Griger, F.; Hartmann, J.; Jiang, G.; Moosdorf, N.; Richts, A.; Stevanovic, Z., et al. The World Karst Aquifer Mapping project: concept, mapping procedure and map of Europe. *Hydrogeology Journal* **2017**, *25*, 771-785, doi:10.1007/s10040-016-1519-3.

5. Vuille, M.; Burns, S.J.; Taylor, B.L.; Cruz, F.W.; Bird, B.W.; Abbott, M.B.; Kanner, L.C.; Cheng, H.; Novello, V.F. A review of the South American monsoon history as recorded in stable isotopic proxies over the past two millennia. *Clim. Past* **2012**, *8*, 1309-1321, doi:10.5194/cp-8-1309-2012.
6. Cruz, F.W.; Burns, S.J.; Karmann, I.; Sharp, W.D.; Vuille, M.; Cardoso, A.O.; Ferrari, J.A.; Dias, P.L.S.; Viana, O. Insolation-driven changes in atmospheric circulation over the past 116,000 years in subtropical Brazil. *Nature* **2005**, *434*, 63-66.
7. Cruz, F.W.; Karmann, I.; Viana, O.; Burns, S.J.; Ferrari, J.A.; Vuille, M.; Sial, A.N.; Moreira, M.Z. Stable isotope study of cave percolation waters in subtropical Brazil: Implications for paleoclimate inferences from speleothems. *Chemical Geology* **2005**, *220*, 245-262, doi:10.1016/j.chemgeo.2005.04.001.
8. Cruz, F.W.; Vuille, M.; Burns, S.J.; Wang, X.; Cheng, H.; Werner, M.; Lawrence Edwards, R.; Karmann, I.; Auler, A.S.; Nguyen, H. Orbitally driven east–west antiphasing of South American precipitation. *Nature Geoscience* **2009**, *2*, 210-214, doi:10.1038/ngeo444.
9. Bernal, J.P.; Cruz, F.W.; Stríkis, N.M.; Wang, X.; Deininger, M.; Catunda, M.C.A.; Ortega-Obregón, C.; Cheng, H.; Edwards, R.L.; Auler, A.S. High-resolution Holocene South American monsoon history recorded by a speleothem from Botuverá Cave, Brazil. *Earth and Planetary Science Letters* **2016**, *450*, 186-196, doi:http://dx.doi.org/10.1016/j.epsl.2016.06.008.
10. Wang, X.; Auler, A.S.; Edwards, R.L.; Cheng, H.; Ito, E.; Solheid, M. Interhemispheric anti-phasing of rainfall during the last glacial period. *Quaternary Science Reviews* **2006**, *25*, 3391-3403, doi:http://dx.doi.org/10.1016/j.quascirev.2006.02.009.
11. Wang, X.; Auler, A.S.; Edwards, R.L.; Cheng, H.; Ito, E.; Wang, Y.; Kong, X.; Solheid, M. Millennial-scale precipitation changes in southern Brazil over the past 90,000 years. *Geophysical Research Letters* **2007**, *34*, doi:10.1029/2007GL031149.
12. Reuter, J.; Stott, L.; Khider, D.; Sinha, A.; Cheng, H.; Edwards, R.L. A new perspective on the hydroclimate variability in northern South America during the Little Ice Age. *Geophysical Research Letters* **2009**, *36*, doi:10.1029/2009GL041051.
13. Apaéstegui, J.; Cruz, F.W.; Vuille, M.; Fohlmeister, J.; Espinoza, J.C.; Sifeddine, A.; Strikis, N.; Guyot, J.L.; Ventura, R.; Cheng, H., et al. Precipitation changes over the eastern Bolivian Andes inferred from speleothem (δ18O) records for the last 1400 years. *Earth and Planetary Science Letters* **2018**, *494*, 124-134, doi:https://doi.org/10.1016/j.epsl.2018.04.048.
14. Lachniet, M.S.; Burns, S.J.; Piperno, D.R.; Asmerom, Y.; Polyak, V.J.; Moy, C.M.; Christenson, K. A 1500-year El Niño/Southern Oscillation and rainfall history for the Isthmus of Panama from speleothem calcite. *Journal of Geophysical Research: Atmospheres* **2004**, *109*, doi:10.1029/2004JD004694.
15. Cheng, H.; Sinha, A.; Cruz, F.W.; Wang, X.; Edwards, R.L.; d'Horta, F.M.; Ribas, C.C.; Vuille, M.; Stott, L.D.; Auler, A.S. Climate change patterns in Amazonia and biodiversity. *Nature Communications* **2013**, *4*, 1411, doi:10.1038/ncomms2415

https://www.nature.com/articles/ncomms2415 - supplementary-information.

16. Van Breukelen, M.R.; Vonhof, H.B.; Hellstrom, J.C.; Wester, W.C.G.; Kroon, D. Fossil dripwater in stalagmites reveals Holocene temperature and rainfall variation in Amazonia. *Earth and Planetary Science Letters* **2008**, *275*, 54-60.
17. Novello, V.F.; Vuille, M.; Cruz, F.W.; Stríkis, N.M.; de Paula, M.S.; Edwards, R.L.; Cheng, H.; Karmann, I.; Jaqueto, P.F.; Trindade, R.I.F., et al. Centennial-scale solar forcing of the South American Monsoon System recorded in stalagmites. *Scientific Reports* **2016**, *6*, 24762, doi:10.1038/srep24762

https://www.nature.com/articles/srep24762 - supplementary-information.

18. Novello, V.F.; Cruz, F.W.; Karmann, I.; Burns, S.J.; Stríkis, N.M.; Vuille, M.; Cheng, H.; Lawrence Edwards, R.; Santos, R.V.; Frigo, E., et al. Multidecadal climate variability in Brazil's Nordeste during the last 3000 years based on speleothem isotope records. *Geophysical Research Letters* **2012**, *39*, doi:10.1029/2012GL053936.

19. Kanner, L.C.; Burns, S.J.; Cheng, H.; Edwards, R.L.; Vuille, M. High-resolution variability of the South American summer monsoon over the last seven millennia: insights from a speleothem record from the central Peruvian Andes. *Quaternary Science Reviews* **2013**, *75*, 1-10, doi:http://dx.doi.org/10.1016/j.quascirev.2013.05.008.

20. Novello, V.F.; Cruz, F.W.; Vuille, M.; Stríkis, N.M.; Edwards, R.L.; Cheng, H.; Emerick, S.; de Paula, M.S.; Li, X.; Barreto, E.d.S., et al. A high-resolution history of the South American Monsoon from Last Glacial Maximum to the Holocene. *Scientific Reports* **2017**, *7*, 44267, doi:10.1038/srep44267
https://www.nature.com/articles/srep44267 - supplementary-information.

21. Novello, V.F.; Cruz, F.W.; Moquet, J.S.; Vuille, M.; Paula, M.S.; Nunes, D.; Edwards, R.L.; Cheng, H.; Karmann, I.; Utida, G., et al. Two Millennia of South Atlantic Convergence Zone Variability Reconstructed From Isotopic Proxies. *Geophysical Research Letters* **2018**, *45*, 5045-5051, doi:10.1029/2017GL076838.

22. Stríkis, N.M.; Cruz, F.W.; Cheng, H.; Karmann, I.; Edwards, R.L.; Vuille, M.; Wang, X.; de Paula, M.S.; Novello, V.F.; Auler, A.S. Abrupt variations in South American monsoon rainfall during the Holocene based on a speleothem record from central-eastern Brazil. *Geology* **2011**, *39*, 1075-1078, doi:10.1130/g32098.1.

23. Stríkis, N.M.; Cruz, F.W.; Barreto, E.A.S.; Naughton, F.; Vuille, M.; Cheng, H.; Voelker, A.H.L.; Zhang, H.; Karmann, I.; Edwards, R.L., et al. South American monsoon response to iceberg discharge in the North Atlantic. *Proceedings of the National Academy of Sciences* **2018**.

24. Stríkis, N.M.; Chiessi, C.M.; Cruz, F.W.; Vuille, M.; Cheng, H.; Souza Barreto, E.A.; Mollenhauer, G.; Kasten, S.; Karmann, I.; Edwards, R.L. Timing and structure of Mega-SACZ events during Heinrich Stadial 1. *Geophysical Research Letters* **2015**, *42*, 5477-5484.

25. Schimpf, D.; Kilian, R.; Kronz, A.; Simon, K.; Spotl, C.; Worner, G.; Deininger, M.; Mangini, A. The significance of chemical, isotopic, and detrital components in three coeval stalagmites from the superhumid southernmost Andes (53 degrees S) as high-resolution palaeo-climate proxies. *Quaternary Science Reviews* **2011**, *30*, 443-459.

26. Kanner, L.C.; Burns, S.J.; Cheng, H.; Edwards, R.L. High-Latitude Forcing of the South American Summer Monsoon During the Last Glacial. *Science* **2012**.

27. Apaéstegui, J.; Cruz, F.W.; Sifeddine, A.; Vuille, M.; Espinoza, J.C.; Guyot, J.L.; Khodri, M.; Strikis, N.; Santos, R.V.; Cheng, H., et al. Hydroclimate variability of the northwestern Amazon Basin near the Andean foothills of Peru related to the South American Monsoon System during the last 1600 years. *Clim. Past* **2014**, *10*, 1967-1981, doi:10.5194/cp-10-1967-2014.

28. Wang, X.; Edwards, R.L.; Auler, A.S.; Cheng, H.; Kong, X.; Wang, Y.; Cruz, F.W.; Dorale, J.A.; Chiang, H.-W. Hydroclimate changes across the Amazon lowlands over the past 45,000 years. *Nature* **2017**, *541*, 204, doi:10.1038/nature20787
https://www.nature.com/articles/nature20787 - supplementary-information.

29. Cruz, F.W.; Burns, S.J.; Karmann, I.; Sharp, W.D.; Vuille, M. Reconstruction of regional atmospheric circulation features during the late Pleistocene in subtropical Brazil from oxygen isotope composition of speleothems. *Earth and Planetary Science Letters* **2006**, *248*, 495-507, doi:10.1016/j.epsl.2006.06.019.

30. Bustamante, M.G.; Cruz, F.W.; Vuille, M.; Apaéstegui, J.; Strikis, N.; Panizo, G.; Novello, F.V.; Deininger, M.; Sifeddine, A.; Cheng, H., et al. Holocene changes in monsoon precipitation in the Andes of NE Peru based on δ18O speleothem records. *Quaternary Science Reviews* **2016**, *146*, 274-287, doi:http://dx.doi.org/10.1016/j.quascirev.2016.05.023.

31. Wortham, B.E.; Wong, C.I.; Silva, L.C.R.; McGee, D.; Montañez, I.P.; Troy Rasbury, E.; Cooper, K.M.; Sharp, W.D.; Glessner, J.J.G.; Santos, R.V. Assessing response of local moisture conditions in central Brazil to variability in regional monsoon intensity using speleothem 87Sr/86Sr values. *Earth and Planetary Science Letters* **2017**, *463*, 310-322, doi:https://doi.org/10.1016/j.epsl.2017.01.034.

32. Berbery, E.H.; Barros, V.R. The Hydrologic Cycle of the La Plata Basin in South America. *Journal of Hydrometeorology* **2002**, *3*, 630-645, doi:10.1175/1525-7541(2002)003<0630:THCOTL>2.0.CO;2.

33. Lenters, J.D.; Cook, K.H. On the Origin of the Bolivian High and Related Circulation Features of the South American Climate. *Journal of the Atmospheric Sciences* **1997**, *54*, 656-678, doi:10.1175/1520-0469(1997)054<0656:OTOOTB>2.0.CO;2.

34. Dee, D.P.; Uppala, S.M.; Simmons, A.J.; Berrisford, P.; Poli, P.; Kobayashi, S.; Andrae, U.; Balmaseda, M.A.; Balsamo, G.; Bauer, P., et al. The ERA-Interim reanalysis: configuration and performance of the data assimilation system. *Quarterly Journal of the Royal Meteorological Society* **2011**, *137*, 553-597, doi:10.1002/qj.828.

35. Schneider, U.; Becker, A.; Finger, P.; Anja, M.-C.; Rudolf, B.; Ziese, M. GPCC Full Data Reanalysis Version 6.0 at 1.0°: Monthly Land-Surface Precipitation from Rain-Gauges built on GTS-based and Historic Data. **2011**, 10.5676/DWD_GPCC/FD_M_V6_100, doi:10.5676/DWD_GPCC/FD_M_V6_100.

36. Berger, A.; Loutre, M.F. Insolation values for the climate of the last 10 million years. *Quaternary Science Reviews* **1991**, *10*, 297-317, doi:http://dx.doi.org/10.1016/0277-3791(91)90033-Q.

37. Böhm, E.; Lippold, J.; Gutjahr, M.; Frank, M.; Blaser, P.; Antz, B.; Fohlmeister, J.; Frank, N.; Andersen, M.B.; Deininger, M. Strong and deep Atlantic meridional overturning circulation during the last glacial cycle. *Nature* **2015**, *517*, 73-76.

38. Donohoe, A.; Marshall, J.; Ferreira, D.; Mcgee, D. The relationship between ITCZ location and cross-equatorial atmospheric heat transport: From the seasonal cycle to the Last Glacial Maximum. *Journal of Climate* **2013**, *26*, 3597-3618.

39. Marshall, J.; Donohoe, A.; Ferreira, D.; McGee, D. The ocean's role in setting the mean position of the Inter-Tropical Convergence Zone. *Climate Dynamics* **2013**, *42*, 1967-1979, doi:10.1007/s00382-013-1767-z.

40. Wang, X.; Auler, A.S.; Edwards, R.L.; Cheng, H.; Cristalli, P.S.; Smart, P.L.; Richards, D.A.; Shen, C.-C. Wet periods in northeastern Brazil over the past 210 kyr linked to distant climate anomalies. *Nature* **2004**, *432*, 740, doi:10.1038/nature03067

https://www.nature.com/articles/nature03067 - supplementary-information.

41. North Greenland Ice Core Project, m.; Andersen, K.K.; Azuma, N.; Barnola, J.M.; Bigler, M.; Biscaye, P.; Caillon, N.; Chappellaz, J.; Clausen, H.B.; Dahl-Jensen, D., et al. High-resolution record of Northern Hemisphere climate extending into the last interglacial period. *Nature* **2004**, *431*, 147, doi:10.1038/nature02805

https://www.nature.com/articles/nature02805 - supplementary-information.

42. Chiang, J.C.H.; Friedman, A.R. Extratropical Cooling, Interhemispheric Thermal Gradients, and Tropical Climate Change. *Annual Review of Earth and Planetary Sciences, Vol 40* **2012**, *40*, 383-412, doi:10.1146/annurev-earth-042711-105545.

43. Dansgaard, W.; Johnsen, S.J.; Clausen, H.B.; Dahl-Jensen, D.; Gundestrup, N.S.; Hammer, C.U.; Hvidberg, C.S.; Steffensen, J.P.; Sveinbjörnsdottir, A.E.; Jouzel, J., et al. Evidence for general instability of past climate from a 250-kyr ice-core record. *Nature* **1993**, *364*, 218, doi:10.1038/364218a0.

44. Petit, J.R.; Jouzel, J.; Raynaud, D.; Barkov, N.I.; Barnola, J.M.; Basile, I.; Bender, M.; Chappellaz, J.; Davis, M.; Delaygue, G., et al. Climate and atmospheric history of the past 420,000 years from the Vostok ice core, Antarctica. *Nature* **1999**, *399*, 429, doi:10.1038/20859

https://www.nature.com/articles/20859 - supplementary-information.

45. Bond, G.; Kromer, B.; Beer, J.; Muscheler, R.; Evans, M.N.; Showers, W.; Hoffmann, S.; Lotti-Bond, R.; Hajdas, I.; Bonani, G. Persistent solar influence on North Atlantic climate during the Holocene. *Science* **2001**, *294*, 2130-2136, doi:10.1126/science.1065680.

46. Gingele, F.X. Holocene climatic optimum in Southwest Africa—evidence from the marine clay mineral record. *Palaeogeography, Palaeoclimatology, Palaeoecology* **1996**, *122*, 77-87, doi:https://doi.org/10.1016/0031-0182(96)00076-4.

47. Liu, F.; Feng, Z. A dramatic climatic transition at ~4000 cal. yr BP and its cultural responses in Chinese cultural domains. *The Holocene* **2012**, *22*, 1181-1197, doi:10.1177/0959683612441839.

48. Cruz, F.W.; Burns, S.J.; Jercinovic, M.; Karmann, I.; Sharp, W.D.; Vuille, M. Evidence of rainfall variations in Southern Brazil from trace element ratios (Mg/Ca and Sr/Ca) in a Late Pleistocene stalagmite. *Geochimica et Cosmochimica Acta* **2007**, *71*, 2250-2263, doi:10.1016/j.gca.2007.02.005.

49. Bird, B.W.; Abbott, M.B.; Vuille, M.; Rodbell, D.T.; Stansell, N.D.; Rosenmeier, M.F. A 2,300-year-long annually resolved record of the South American summer monsoon from the Peruvian Andes. *Proceedings of the National Academy of Sciences* **2011**, *108*, 8583.

50. Cheng, H.; Fleitmann, D.; Edwards, R.L.; Wang, X.; Cruz, F.W.; Auler, A.S.; Mangini, A.; Wang, Y.; Kong, X.; Burns, S.J., et al. Timing and structure of the 8.2 kyr B.P. event inferred from δ18O records of stalagmites from China, Oman, and Brazil. *Geology* **2009**, *37*, 1007-1010, doi:10.1130/G30126A.1.

51. Cruz, F.W.; Burns, S.J.; Karmann, I.; Sharp, W.D.; Vuille, M.; Ferrari, J.A. A stalagmite record of changes in atmospheric circulation and soil processes in the Brazilian subtropics during the Late Pleistocene. *Quaternary Science Reviews* **2006**, *25*, 2749-2761, doi:10.1016/j.quascirev.2006.02.019.

52. Jaqueto, P.; Trindade, R.I.F.; Hartmann, G.A.; Novello, V.F.; Cruz, F.W.; Karmann, I.; Strauss, B.E.; Feinberg, J.M. Linking speleothem and soil magnetism in the Pau d'Alho cave (central South America). *Journal of Geophysical Research: Solid Earth* **2016**, *121*, 7024-7039, doi:10.1002/2016JB013541.

53. Deininger, M.; McDermott, F.; Mudelsee, M.; Werner, M.; Frank, N.; Mangini, A. Coherency of late Holocene European speleothem δ18O records linked to North Atlantic Ocean circulation. *Climate Dynamics* **2017**, *49*, 595-618, doi:10.1007/s00382-016-3360-8.